

AD-A156 651

AN ALGORITHM FOR ACTIVE ADAPTIVE CONTROL OF PERIODIC
INTERFERENCE(U) DAVID W TAYLOR NAVAL SHIP RESEARCH AND
DEVELOPMENT CENTER BETHESDA MD R D PIERCE MAY 85

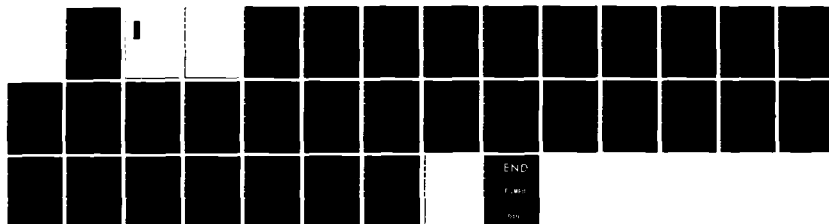
1/1

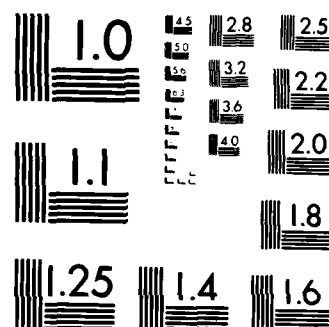
UNCLASSIFIED

/DTNSRDC-85/047

F/G 12/1

NL





MICROCOPY RESOLUTION TEST CHART
NATIONAL BUREAU OF STANDARDS-1963-A

UNCLASSIFIED

SECURITY CLASSIFICATION OF THIS PAGE

AD-A156651

REPORT DOCUMENTATION PAGE

1a. REPORT SECURITY CLASSIFICATION UNCLASSIFIED			1b. RESTRICTIVE MARKINGS		
2a. SECURITY CLASSIFICATION AUTHORITY			3. DISTRIBUTION / AVAILABILITY OF REPORT APPROVED FOR PUBLIC RELEASE: DISTRIBUTION UNLIMITED		
2b. DECLASSIFICATION / DOWNGRADING SCHEDULE			5. MONITORING ORGANIZATION REPORT NUMBER(S)		
4. PERFORMING ORGANIZATION REPORT NUMBER(S) DTNSRDC-85/047			7a. NAME OF MONITORING ORGANIZATION		
6a. NAME OF PERFORMING ORGANIZATION David Taylor Naval Ship R&D Center		6b. OFFICE SYMBOL (If applicable) Code 2960		7b. ADDRESS (City, State, and ZIP Code)	
6c. ADDRESS (City, State, and ZIP Code) Bethesda, Maryland 20084-5000		8a. NAME OF FUNDING / SPONSORING ORGANIZATION		8b. OFFICE SYMBOL (If applicable)	
8c. ADDRESS (City, State, and ZIP Code)		9. PROCUREMENT INSTRUMENT IDENTIFICATION NUMBER			
11 TITLE (Include Security Classification) AN ALGORITHM FOR ACTIVE ADAPTIVE CONTROL OF PERIODIC INTERFERENCE		10. SOURCE OF FUNDING NUMBERS			
		PROGRAM ELEMENT NO. 61152N		PROJECT NO. R00001	
		TASK NO. ZR0110801		WORK UNIT ACCESSION NO. DN378297	
12 PERSONAL AUTHOR(S) Pierce, Robert Dorrington					
13a. TYPE OF REPORT Final		13b. TIME COVERED FROM _____ TO _____		14. DATE OF REPORT (Year, Month, Day) 1985, May	
15. PAGE COUNT 32					
16 SUPPLEMENTARY NOTATION					
17 COSATI CODES			18. SUBJECT TERMS (Continue on reverse if necessary and identify by block number)		
FIELD	GROUP	SUB-GROUP	Active control, adaptive, antinoise.		
19 ABSTRACT (Continue on reverse if necessary and identify by block number)					
<p>An algorithm is presented for the active adaptive control of periodic interference. This algorithm is derived, its performance is theoretically analyzed, and the algorithm and its performance are verified by laboratory experiments. In these experiments, this control method is shown to reduce the periodic components by more than 40 dB.</p>					
20 DISTRIBUTION / AVAILABILITY OF ABSTRACT <input checked="" type="checkbox"/> UNCLASSIFIED/UNLIMITED <input type="checkbox"/> SAME AS RPT. <input type="checkbox"/> DTIC USERS			21. ABSTRACT SECURITY CLASSIFICATION UNCLASSIFIED		
22a. NAME OF RESPONSIBLE INDIVIDUAL Robert Dorrington Pierce			22b. TELEPHONE (Include Area Code) (202) 227-1591		22c. OFFICE SYMBOL Code 2960

TABLE OF CONTENTS

	Page
LIST OF FIGURES	iii
ABSTRACT	1
ADMINISTRATIVE INFORMATION	1
INTRODUCTION	1
THE CONTROL ALGORITHM	2
DERIVATION OF THE ALGORITHM	2
THEORETICAL SOLUTION OF THE ALGORITHM	6
MISADJUSTMENT IN NOISE	8
CONVERGENCE RATE	10
ESTIMATION OF THE CONTROL LOOP FILTER MATRIX	11
LABORATORY EXPERIMENT	11
CONFIGURATION	11
IMPLEMENTATION OF THE ALGORITHM	13
RESULTS	14
CONCLUSIONS	18
ACKNOWLEDGMENTS	18
APPENDIX - COVARIANCE OF FOURIER SERIES COEFFICIENTS WHEN APPLYING SIGNAL AVERAGING	19
REFERENCES	27

LIST OF FIGURES

1 - Control System for Active Adaptive Control	4
2 - Experimental Configuration	12
3 - Final Levels of Interference Reduction for Accelerometer 1, $\eta = 0.35$ and $M = 10$	15

	Page
4 - Final Levels of Interference Reduction for Accelerometer 2, $\eta = 0.35$ and $M = 10$	15
5 - Final Levels of Interference Reduction for Residual Accelerometer, $\eta = 0.35$ and $M = 10$	16
6 - An Example of Misadjustment for Accelerometer 1, $\eta = 1.0$ and $M = 5$	16
7 - Misadjustment Signal Plus Noise-to-Noise Ratio for Accelerometer 1 and the 86.8 Hertz Component	17
8 - Average Number of Iterations Required to Reach 20 Decibels of Interference Reduction	17
A.1 - $\sin(x)/x$ Filter for $M = 4$ Superimposed on Noise Autospectrum	23
A.2 - Coefficient Variance for First Harmonic	25
A.3 - Coefficient Variance for Second Harmonic	26

ABSTRACT

An algorithm is presented for the active adaptive control of periodic interference. This algorithm is derived, its performance is theoretically analyzed, and the algorithm and its performance are verified by laboratory experiments. In these experiments, this control method is shown to reduce the periodic components by more than 40 dB.

ADMINISTRATIVE INFORMATION

This work was sponsored by the David Taylor Naval Ship Research and Development Center's (DTNSRDC) Independent Research Program under Task ZR0110801, Program Element 61152N, and Work Unit 1965-139.

INTRODUCTION

The objective of active adaptive control is the cancellation or minimization of a physical quantity such as acoustic noise or mechanical vibration by physically generating a controlled cancellation stimulus that will destructively superimpose with the physical quantity produced by the interfering source. Since many sources of noise or vibration are periodic in nature (rotating machinery, for example), the control algorithm of only this class of interfering sources is considered in this report. An excellent overview article that describes the application and results of this type of control is given by Chaplin.^{1*} This article, as well as other papers in the literature, such as Kosaka, et al.,² and Smith and Chaplin,³ however, do not reveal very many details of how their algorithms function.

Smith and Chaplin³ describe three basic types of adaptation algorithms: power sensing, waveform sensing, and transform method. In the power sensing method, the cycle is divided into N segments and the amplitude of each time segment in the cancellation signal is adjusted until the error signal power averaged over a complete cycle is minimized. The waveform sensing method uses the error amplitude at its corresponding cancellation signal time segment (compensation for time delay) to adjust the cancellation signal until the error signal is minimized. The transform method operates in the frequency domain; the transfer function between the cancellation signal and the error signal is

* A complete listing of references is given on page 27.

characterized and a cancellation signal is developed that minimizes the error signal. With each of these methods, a synchronization signal (tachometer, for example) is used to control timing in the algorithm. Noise immunity is enhanced by applying signal averaging procedures (synchronous averaging over a number of cycles).

The control algorithm presented in this report uses the transform method combined with signal averaging procedures. This algorithm is derived for the general case of multiple control loops such that cross-coupling between each actuator and sensor is included. It's performance is theoretically analyzed to determine the influence of algorithm parameters on the convergence rate and loop misadjustment in the presence of noise. Also presented are the results of applying this algorithm to a laboratory experiment involving vibration on a beam that is supported and controlled at two points.

The application of this control method to different situations will require a case-by-case analysis of the physical system. The interference levels measured by the sensors (the measured error signals) are reduced using this method; however, at other locations, the interference levels could actually be increased (a nonrigid body, for example). The actuators and sensors must be correctly located to achieve global reduction of these levels. Determining these locations requires a careful study and understanding of the different modes or degrees-of-freedom present in the actual structure or sound field.

THE CONTROL ALGORITHM

DERIVATION OF THE ALGORITHM

The derivation of the active adaptive control algorithm for periodic interference begins with a description and understanding of the constraints imposed by the control problem. First, synchronization between the interfering and cancellation signals is required. For rotating machinery, a tachometer or shaft position encoder can provide this synchronization. Next are the factors that distinguish this control problem from the normal realm of feedback and control: Only the sum of the interfering and cancellation signals is measurable -- the error signal of the feedback loop. The cancellation signal propagates in the medium and will prevent the measurement of only the interfering signal. Also, mechanical and electronic filters are present within

the feedback loop. Linear filters are assumed; however, antialiasing filters, transducers, and signal propagation in the medium will produce the frequency dependent gain and phase variations that define this filter within the control loop.

The control algorithm operates in the frequency domain. The Fourier series components of the error signal are obtained using the Fast Fourier Transform (FFT); these components are processed to produce the next iteration of the cancellation signal's Fourier series. Synchronization preserves the phase relationships of the Fourier series components. The time domain samples for the cancellation signal are produced using the inverse FFT. The algorithm is adaptive in the sense that it will track time varying changes in the amplitude and phase of the periodic interference. However, the filter in the feedback loop is not "self-designing." Prior to the adaptation process, a model of the control loop filter is estimated. If the control loop becomes unstable, then the adaptation process would be halted, the control loop filter reestimated, and the adaptation process begun again.

The block diagram of the control system in the frequency domain is given in Figure 1. The description of each term is given as follows:

$A(\omega_j)$	Interference Signal Vector
$N(\omega_j)$	Noise Signal Vector
$B(\omega_j)$	Cancellation Signal Vector
$E(\omega_j)$	Error Signal Vector
$D(\omega_j)$	Control Loop Filter Matrix
$C(\omega_j)$	Measured Error Signal Vector

where $\omega_j = (j-1)\omega_f$, $\omega_f = 2\pi/(JT)$ is the fundamental frequency, $1 \leq j \leq (J/2)-1$, T is the time between samples, and J is the number of samples in the period JT . Except when necessary, the functional dependence on ω_j is not included in the equations presented in the rest of this report; this dependence is assumed unless otherwise stated. For Q control loops, each signal vector contains Q elements and the control loop filter matrix is a Q by Q matrix that includes the cross-coupling between each cancellation signal and each measured error signal. In this model, only the error signal vector, C , is measurable. The

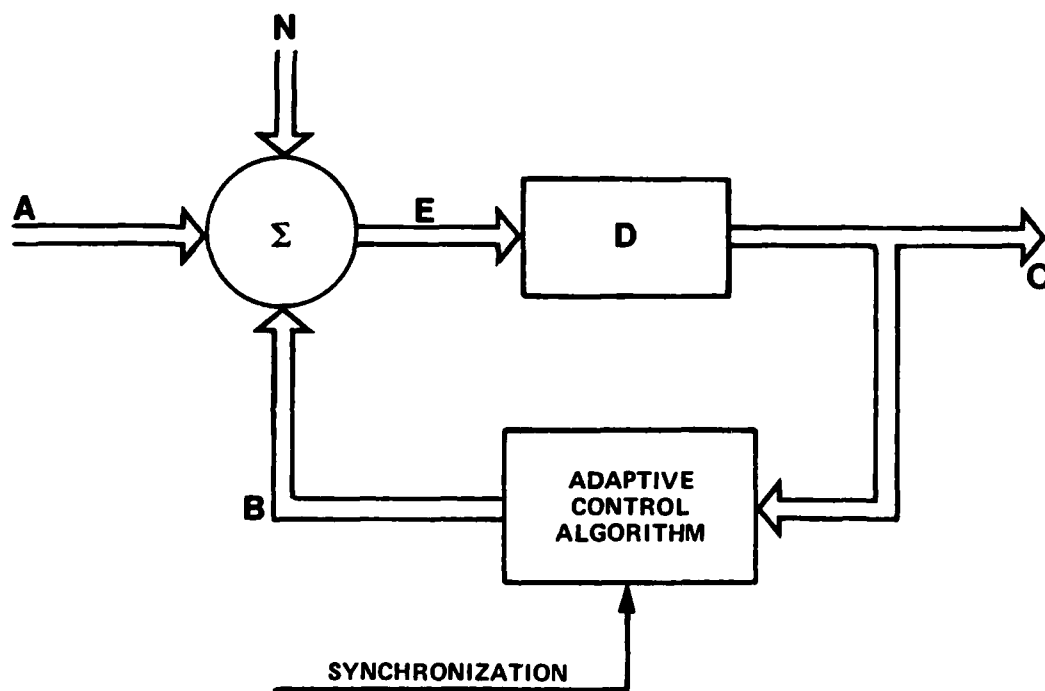


Figure 1 - Control System for Active Adaptive Control

control loop filter matrix, D , is the product of all filters between each cancellation signal and each measured error signal (mechanical, antialiasing, transducers, signal propagation, etc.). The noise signal vector, N , can consist of random noise, as well as other unsynchronized periodic signals.

The matrix equation for the control loop is

$$C = D (A + N + B) \quad (1)$$

where A and N are unknown, and B is the independent variable. Since D is measured, the error signal vector, E , is given by the inverse matrix equation:

$$E = D^{-1} C \quad (2)$$

where

$$E = A + N + B \quad (3)$$

The inverse matrix of the control loop filter is assumed to exist; locating the actuators and sensors to achieve this condition is a major requirement in applying this control method. The performance surface for the control algorithm is given by the error signal power, $P(B)$. For the n^{th} control loop,

$$P_n(B_n) = E_n^* E_n \quad (4)$$

The control algorithm uses gradient search techniques; see Widrow and Stearns.⁴ The $k+1$ iteration of the cancellation signal, $B(k+1)$, is based on the last iteration and the negative gradient of the performance surface. The minimum of this parabolic surface is being sought. So,

$$B(k+1) = B(k) + \mu [-\nabla(k)] \quad (5)$$

where μ is the adaptation parameter that sets convergence speed and loop

stability. For the n^{th} control loop, the gradient is

$$\nabla_n(k) = \left. \frac{\partial P_n}{\partial B_n} \right|_{B_n=B_n(k)} = 2 E_n \quad (6)$$

The adaptation equation becomes

$$B(k+1) = B(k) - \eta E(k) \quad (7)$$

where the adaptation parameter is redefined as $\eta = 2\mu$. Since independent estimates of the gradient do not exist, the LMS (least mean squares) approach is taken; see Widrow and Stearns.⁴ The current error, $E(k)$, (estimated by using the measured error vector and the inverse of the measured control loop filter matrix in Equation (2)) is used for the gradient. Note that all cross-coupling is eliminated; the individual signals in each vector are now independent of one another. In the following equations, the matrix notation is dropped unless otherwise noted; relationships presented for a single control loop will apply for all control loops.

THEORETICAL SOLUTION OF THE ALGORITHM

The adaptation equation, Equation (7), is a linear, first-order, constant-coefficient, ordinary difference equation (see Widrow and Stearns⁴). This equation is solved by induction from the first several iterations. Assuming that the control signal is initially zero, the control signal at the k^{th} iteration is

$$B(k) = -A + (1-\eta)^k A - \eta \sum_{j=0}^{k-1} N(j) (1-\eta)^j \quad (8)$$

This equation is stable provided the geometric ratio, r , is

$$|r| = |1 - \eta| < 1 \quad (9)$$

For $0 < \eta < 1$, the adaptation equation is overdamped; it is critically damped for $\eta = 1$, and underdamped for $1 < \eta < 2$.

From Equations (3) and (8), the error signal solution is

$$E(k) = (1-\eta)^k A + N(k) - \eta \sum_{j=0}^{k-1} N(j) (1-\eta)^j \quad (10)$$

The mean and variance of the error signal are derived under the assumptions that the noise signal is a complex random variable with zero mean and stationary parameters. Its variance is σ_N^2 . Since overlapped estimates of the coefficients are not made (see the Appendix), the covariance is zero ($E[N^*(j)N(k)] = 0$, for $j \neq k$, where $E[\cdot]$ is the expected value operator.) For zero mean noise, the mean value of the error signal is

$$E[E(k)] = (1-\eta)^k A \quad (11)$$

The variance of the error signal is

$$\text{VAR}[E(k)] = \sigma_N^2 + \sigma_N^2 \eta / (2-\eta) - \sigma_N^2 \eta (1-\eta)^{2k} / (2-\eta) \quad (12)$$

The average learning curve for the algorithm is given by the expected value of the error signal power. From Equations (4), (11) and (12), the average error signal power for the k^{th} iteration is

$$E[P(k)] = (1-\eta)^{2k} A^* A - \sigma_N^2 \eta (1-\eta)^{2k} / (2-\eta) + \sigma_N^2 + \sigma_N^2 \eta / (2-\eta) \quad (13)$$

The first two terms of Equation (13) are functions of the k^{th} iteration; for a geometric ratio chosen within the limits of stability, these terms will converge to zero as k increases; this is the transient response of the loop. Once the loop converges, the last two terms limit the depth of the convergence. The σ_N^2 term is due to the noise present from the k^{th} iteration, and the last term is defined as the misadjustment, M , that is due to the influence of noise

present during the last $k-1$ iterations:

$$M = \sigma_N^2 \eta / (2-\eta) \quad (14)$$

MISADJUSTMENT IN NOISE

Once the algorithm has converged, an important measure of the algorithms performance is its misadjustment in noise. As shown in Equation (13), the depth of convergence is limited by the noise. When the autospectrum of the measured error signal is viewed on a spectrum analyzer, the individual components generally stand out above the noise autospectrum. In the following derivation, this misadjustment is expressed as a signal plus noise to noise ratio that can be easily measured using a spectrum analyzer with appropriate spectral resolution.

This derivation follows the steps performed by the algorithm. First, signal averaging is used to reduce the influence of the noise in the measured error signal, then the complex Fourier series coefficients are calculated using the Discrete Fourier Transform (DFT) (The computer algorithm for this procedure is the Fast Fourier Transform (FFT).) The noise variance vector transformed to the measured error signal, $D\sigma_N^2$, is the variance of these Fourier coefficients; this variance, as derived in the Appendix, is:

$$D\sigma_N^2 = S_{nn}(\omega_j) \omega_f / (2M) \quad (15)$$

where $S_{nn}(\omega_j)$ is the autospectrum of the noise in the measured error signal vector, ω_f is the fundamental frequency in radians/second, and M is the number of cycles averaged. The variance is the autospectrum of the noise at each harmonic multiplied by the bandwidth between each harmonic and divided by two times the number of cycles averaged. From Equation (14), the misadjustment transformed to the measured error signal for each control loop becomes

$$M(\omega_j) = [\eta / (2-\eta)] S_{nn}(\omega_j) [\omega_f / (2M)] \quad (16)$$

Once an iteration of the algorithm has been performed, the coefficients are transformed back into the time domain and this misadjustment is held

constant (sinusoidal signals) until the results from the next iteration are transferred to the output. This time delay is necessary to allow the transient response to the last iteration to settle to a steady-state value. Also, time is required to perform the M signal averages and to process these averages for the next iteration. This time delay is expressed as the number of cycles, $M + F$, that the periodic signal undergoes between iterations. During an iteration, M is the number of cycles averaged and F is the fixed number of cycles required to await steady-state and to do the necessary processing. Since the noise is assumed to be statistically uncorrelated from one iteration to the next, the misadjustment signal looks like a series of sinusoids with amplitudes and phases that randomly change every $M + F$ cycles. Hence, the misadjustment signal is a sum of narrow-band random processes where the autospectrum at each ω_j is a sine wave convolved with a rectangular window that is $J(M+F)$ samples long. The expected value of this misadjustment spectrum, $S_{MM}(\omega_j)$, is

$$S_{MM}(\omega_j) = M(\omega_j) (M+F)JT/\pi \quad (17)$$

So,

$$S_{MM}(\omega_j) = [\eta/(2-\eta)] [(M+F)/M] S_{nn}(\omega_j) \quad (18)$$

When a spectrum analyzer is connected to the measured error signal, this estimated spectrum will contain the misadjustment spectrum plus the noise spectrum. The misadjustment expressed as the signal plus noise to noise ratio, $SNNR_M$, in dB is defined as

$$SNNR_M = 10 \log\{[S_{MM}(\omega_j) + S_{nn}(\omega_j)]/S_{nn}(\omega_j)\} \quad (19)$$

for each measured error signal at each ω_j . So,

$$SNNR_M = 10 \log\{1 + [\eta/(2-\eta)](M+F)/M\} \quad (20)$$

Since $(M+F)/M$ is always greater than one, signal averaging helps to reduce the "cost" of requiring a fixed time to await steady-state and to do the signal processing. For example: if $F = 8$ and $M = 1$ (no averaging), then $(M+F)/M$ is 9;

and if $M = 10$, then $(M+F)/M$ is 1.8. Averaging 10 cycles compared to no averaging yields a 7 dB improvement in misadjustment; averaging 100 cycles, however, produces only an additional 2.2 dB improvement. Reducing the value of the adaptation parameter, η , will also reduce misadjustment. The cost of reduced misadjustment is time; signal averaging takes time, and small values for the adaptation parameter, η , will increase the time required to reduce the interference to a particular level.

To avoid bias error when viewing the misadjustment on a spectrum analyzer, the spectral resolution of the analyzer should be narrower than the bandwidth of the misadjustment spectrum. As $M + F$ increases, this spectrum becomes narrower and narrower. The half-power bandwidth of this spectrum is approximately $1/((M+F)JT)$ hertz.

CONVERGENCE RATE

The convergence rate is another important measure of the algorithms' performance. When the interference signal power, A^*A , is much larger than the noise variance, σ_N^2 , the convergence rate is controlled by the first term in Equation (13). Using this term, the average number of iterations, k_{20} , required to reduce the magnitude of the error signal by 20 dB is

$$k_{20} = -1/\log_{10}(1-\eta) \quad (21)$$

For $\eta = 0.9$, a reduction of 20 dB is reached in one iteration; for $\eta = 0.1$, 22 iterations are required. Note that all harmonics will converge at the same rate. The average time required (in seconds) to reach this level of convergence, T_c , is

$$T_c = (M+F)k_{20}/f_p \quad (22)$$

where f_p is the fundamental frequency in hertz.

ESTIMATION OF THE CONTROL LOOP FILTER MATRIX

The control loop filter matrix, D , is estimated prior to adaptation by changing one control signal at a time and storing the change in the measured error signal vector. Assuming that the interference signal vector is constant during this calibration sequence, the change in the measured error signal vector is given by:

$$C(k) - C(k-1) = D[A+N(k)+B(k)] - D[A+N(k-1)+B(k-1)] \quad (23)$$

The interference signal vector is eliminated, so

$$\Delta C = D (\Delta N + \Delta B) \quad (24)$$

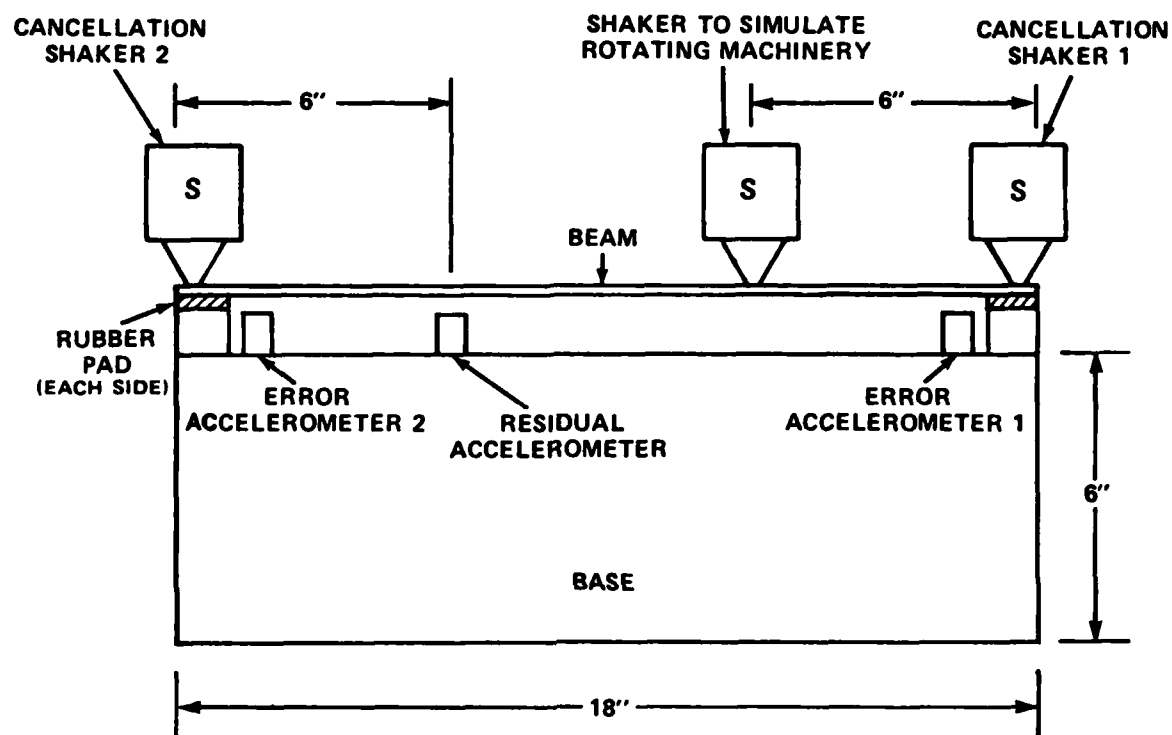
The influence of the noise is already reduced by using signal averaging on the measured error time history prior to transformation to the frequency domain. Additional reduction in the influence of the noise is possible by repeating the calibration process and averaging the results in the frequency domain. Since only one control signal is varied at a time, the column elements of the control loop filter matrix are then estimated by the ratio of the two frequency domain averages:

$$D_{pq} = \frac{\langle \Delta C_p \Delta B_q^* \rangle}{\langle \Delta B_q \Delta B_q^* \rangle} \quad (25)$$

LABORATORY EXPERIMENT

CONFIGURATION

As shown in Figure 2, the active adaptive control experiment was conducted using a beam supported at both ends with rubber mounts. An interference source was simulated by a shaker that was offset from the center of the beam. Two rubber mounts coupled the vibration from the shaker to the base. The base was suspended from a wooden frame with rubber shock cords. Since this shaker was offset from center, vertical and rotational vibration was induced into the base; the solid base was a rigid body at the excitation frequencies. Control



NOTES: BASE AND BEAM ARE 2 INCHES DEEP.
BEAM IS 1/4 INCH THICK.

Figure 2 - Experimental Configuration

shakers were located on each end of the beam just above each mount. The resultant or error vibration was measured using accelerometers on the base and located next to each mount. A third accelerometer was located on the base to measure any residual vibration in the base; this accelerometer was not used with the adaptive control algorithm.

The drive signal for the shaker that simulated the rotating machinery (interference source) was generated by a Digital Equipment Corporation (DEC) PDP 11/73 microcomputer to produce five components of a periodic signal with a fundamental frequency of 86.806 hertz. This microcomputer also provided the signals (a digital word that varied from 0 to 31) to simulate a shaft position encoder. Each cycle was divided into 32 positions. To simulate background noise, bandlimited white noise from an HP3722A noise generator was added to the drive signal from the microcomputer.

The three Wilcoxon F3 electromechanical shakers were driven with Wilcoxon PA7C power amplifiers; the shaker drive signals were filtered by 500 Hz low pass filters. The acceleration on the base was measured using Columbia 302-7A piezoelectric accelerometers that were conditioned by Wilcoxon AM 5 amplifiers. The error signal was also filtered with 500 Hz low pass filters prior to digitization by the analog to digital converter. A Data Translation Model DT2781 analog interface module contained the digital to analog converters used to produce the drive signals, and the analog to digital converters used to sample the error signals; both types of converters have 12 bit resolution.

IMPLEMENTATION OF THE ALGORITHM

The control algorithm was implemented on a second DEC PDP 11/73 microcomputer using a Sky array processor and a mix of assembly language and FORTRAN programming. Under interrupt control, an assembly language program handled the analog input and output, as well as the digital input from the simulated shaft position encoder. An interrupt occurred whenever the shaft position encoder indicated the next shaft position. When each interrupt occurred, the next error signal sample was collected and the next cancellation signal sample was produced by the digital to analog converter. The data samples received from and sent to this assembly program were linked to the FORTRAN program by a common memory block. While these interrupts occurred, this FORTRAN

program worked at its own speed to produce the cancellation signal samples. Once the FORTRAN program produced a new iteration, it would wait a fixed number of cycles until the error signal reached a steady-state condition before sampling the results of this past iteration. When the next complete cycle was sampled, the signal averaging would begin for M cycles. The Fast Fourier Transforms (FFT) and the inverse FFT's were processed by the Sky array processor. The adaptation using the Fourier coefficients was performed with the FORTRAN program steps. Approximately eight cycles of the process occurred while a new iteration was being prepared; the last cancellation signal cycle was repeated during these computations.

RESULTS

The algorithm performed as expected. As shown in Figures 3 and 4, the periodic interference coupled to either end of the base was reduced for almost all harmonics by more than 40 dB. The levels of reduction given in Figure 5 for the off-center or residual accelerometer are slightly less than the levels at the ends of the base. The levels after convergence are just above the imposed background level.

The misadjustment was measured in detail for the 86.8 Hz component. Figure 6 gives an example of large misadjustment when $\eta = 1$ and $M = 5$. The autospectrum of the background noise was estimated at this frequency. The signal plus noise to noise ratio from Equation (20) was evaluated using $F = 8$ cycles to predict the measured level of misadjustment. The results of this comparison are given in Figure 7. For a range of algorithm parameters, the measured misadjustment agrees closely to the level predicted from the measurements of the background noise. For different algorithm parameters, the misadjustment is adequately predicted by Equation (20).

The number of iterations required to achieve a reduction of 20 dB in the interference was measured by averaging this value for each of the five components. As shown in Figure 8, these results are compared to the predicted values from Equation (21) for a range of algorithm parameters. Except for when the adaptation parameter is greater than 0.7, the measured and predicted results agree closely.

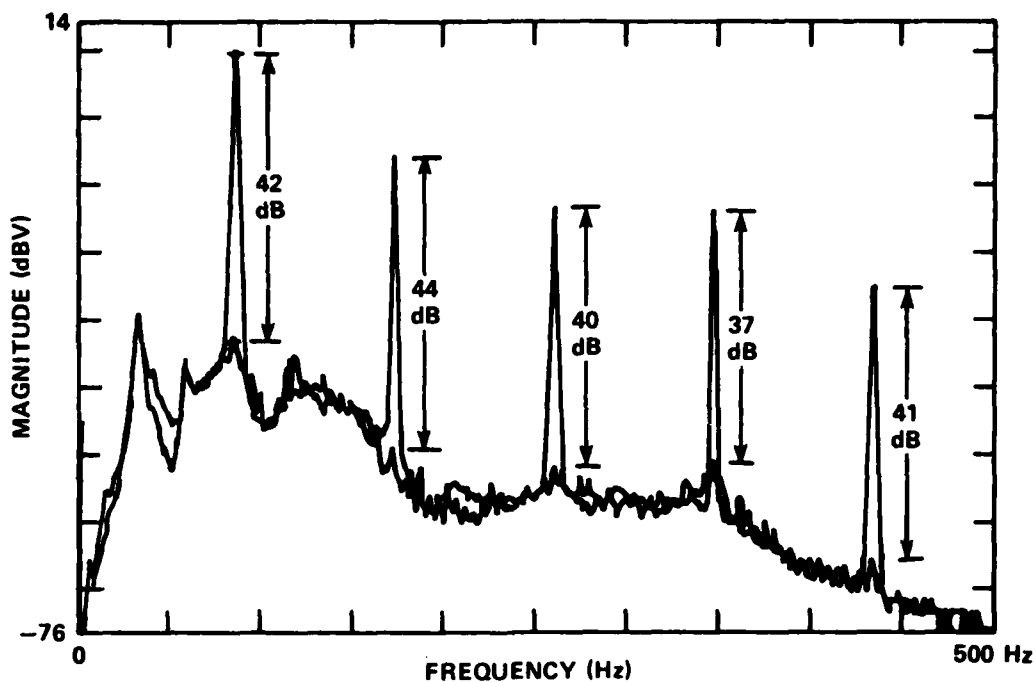


Figure 3 - Final Levels of Interference Reduction for Accelerometer 1, $\eta = 0.35$ and $M = 10$

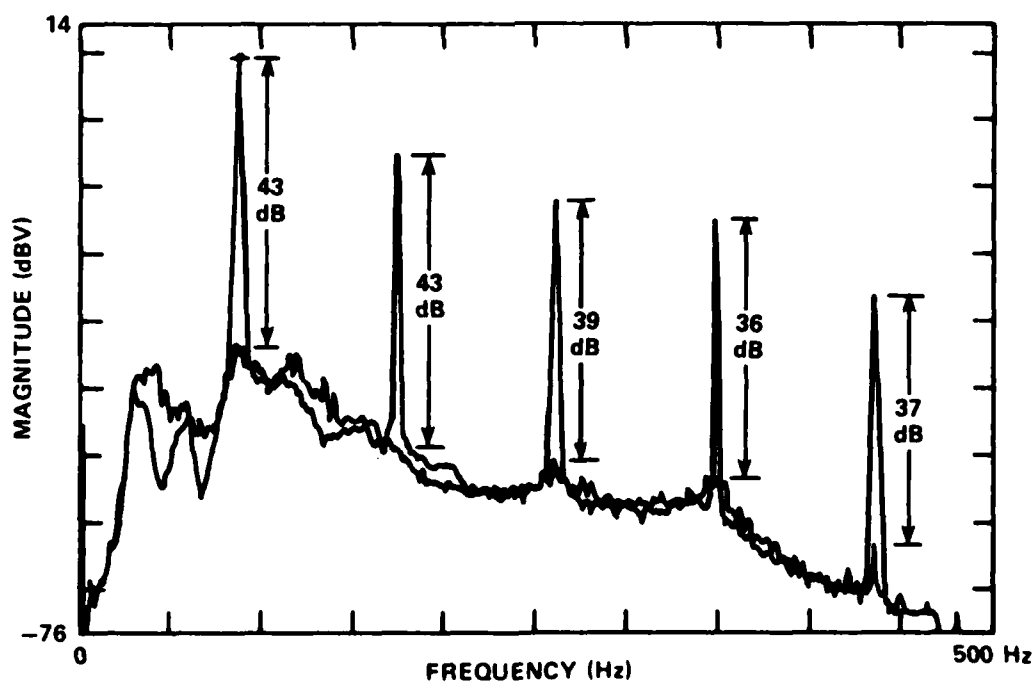


Figure 4 - Final Levels of Interference Reduction for Accelerometer 2, $\eta = 0.35$ and $M = 10$

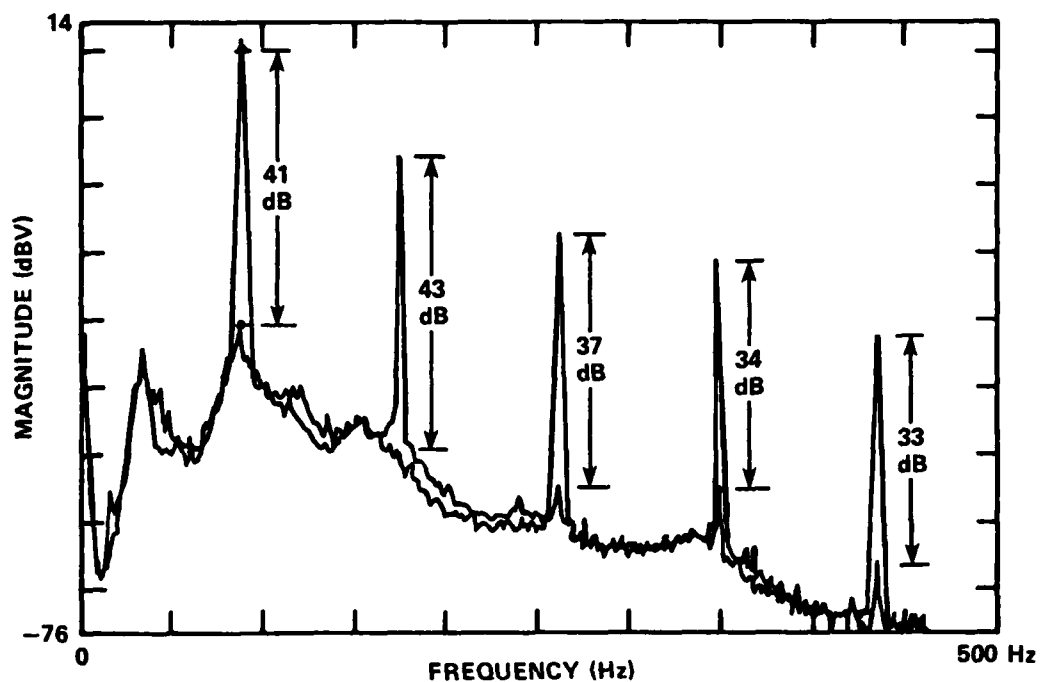


Figure 5 - Final Levels of Interference Reduction for Residual Accelerometer, $\eta = 0.35$ and $M = 10$

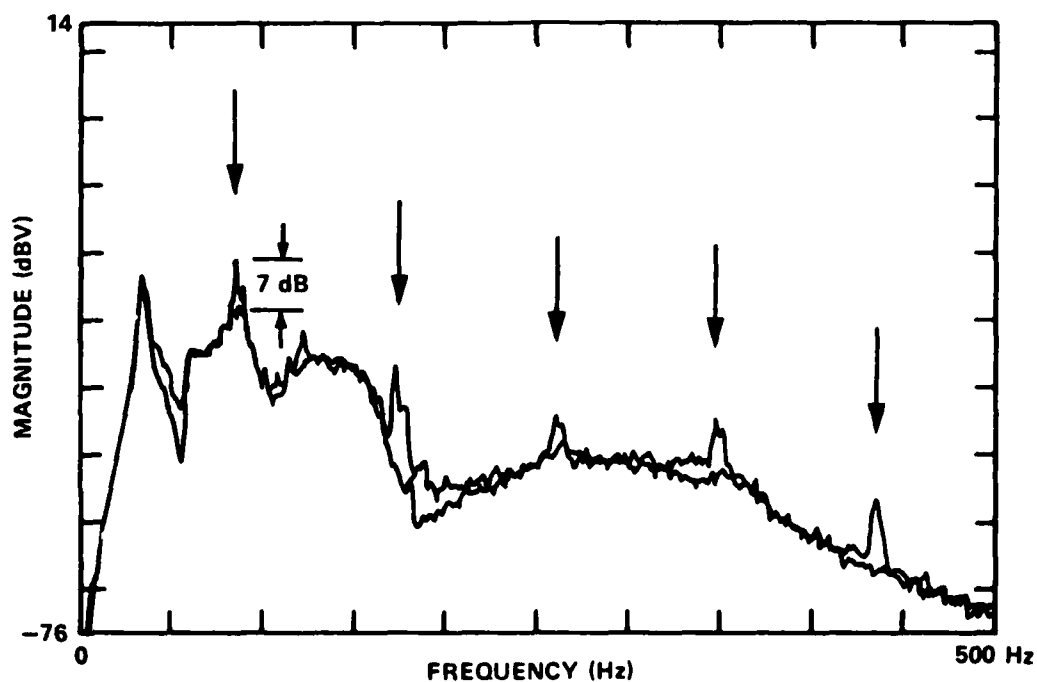


Figure 6 - An Example of Misadjustment for Accelerometer 1, $\eta = 1.0$ and $M = 5$

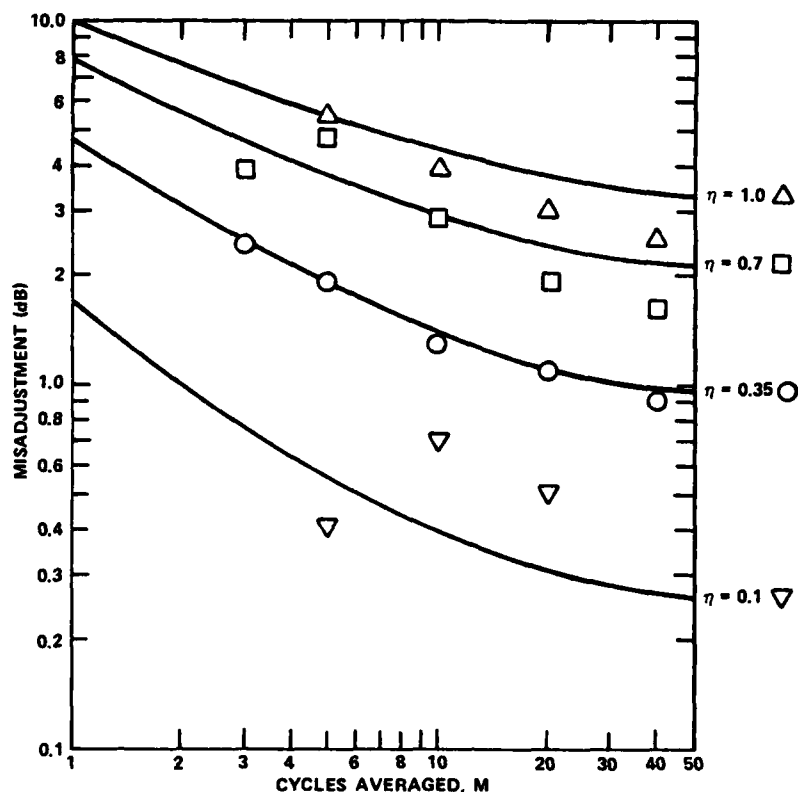


Figure 7 - Misadjustment Signal Plus Noise-to-Noise Ratio for Accelerometer 1 and the 86.8 Hertz Component

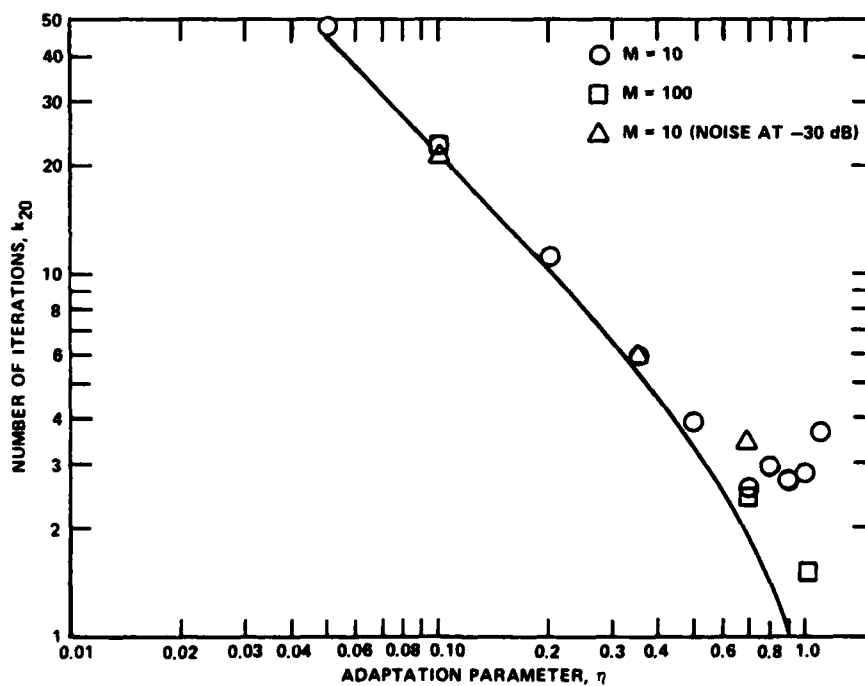


Figure 8 - Average Number of Iterations Required to Reach 20 Decibels of Interference Reduction

CONCLUSIONS

A general method for actively controlling periodic interference is presented. The algorithm works and the major parameters that affect its performance are understood. The method does require prior estimation of the control loop transfer function matrix, and this transfer function is assumed to be constant with little variation with time. Also, the inverse transfer function matrix is assumed to exist; proper location of the actuators and sensors is required to insure existence of this inverse matrix.

ACKNOWLEDGMENTS

Appreciation is extended to Dr. Bruce Douglas, Mr. Roger Evans, and Mr. Robert Ratcliffe (Code 1961) for cooperation and assistance in setting up and conducting the experiments and in evaluating the structural aspects of applying this control method.

Also, appreciation is extended to Mr. John Davies III (Code 2950) for assistance in developing the real time computer systems and software necessary for implementing this control method.

APPENDIX

COVARIANCE OF FOURIER SERIES COEFFICIENTS WHEN APPLYING SIGNAL AVERAGING

Given a periodic signal added to random noise, signal averaging is a standard technique for recovering this periodic signal from the noise. This recovery is not perfect and the affects of the noise are seen when repeated averages of the signal are taken. This lack of repeatability is also present in the Fourier series coefficients for each averaged signal. The variance of these coefficients expresses their statistical variability, and the covariance expresses their joint statistical characteristics. When these coefficients are used as part of a signal processing algorithm, for example, the covariance is useful in defining the performance of this algorithm. This variance and covariance are now derived; the background noise from the active adaptive control experiment is used as an example.

For a sampled time history, x_q , that contains a periodic signal plus random noise, the q^{th} sample is

$$x_q = p_q + n_q \quad (\text{A.1})$$

where p_q is the periodic signal and n_q is the noise. The period is N samples and the time between each sample is T . The noise is assumed to be a zero mean, stationary random process with an autospectrum of $S_{nn}(\omega)$. After averaging M cycles of the periodic signal, the average signal is

$$c_k(r) = p_k(r) + (1/M) \sum_{m=1}^M n_{(m-1)N+k+r} \quad (\text{A.2})$$

where $1 \leq k \leq N$ and r is the index of the initial sample. The Fourier series

coefficients are estimated using the Discrete Fourier Transform (DFT)

$$C_j(r) = (1/N) \sum_{k=1}^N c_k(r) e^{-i(2\pi/N)(k-1)(j-1)} \quad (A.3)$$

The coefficients for the averaged signal are

$$C_j(r) = P_j(r) + (1/NM) \sum_{m=1}^M \sum_{k=1}^N n_{(m-1)N+k+r} e^{-i(2\pi/N)(k-1)(j-1)} \quad (A.4)$$

The coefficient estimate is a complex random variable. Except for the assumption that the noise is a zero mean, stationary random process, no other assumptions about the noise process are required to derive the mean and covariance of these coefficients. (For M large, however, the probability density function of these coefficients will, from the central limit theorem, approach a Gaussian distribution regardless of the distribution of the noise samples.) Since the noise is zero mean, the mean value of $C_j(r)$ is

$$E[C_j(r)] = P_j(r) \quad (A.5)$$

where $E[\cdot]$ is the expected value operator. The covariance of two coefficient estimates from two data sequences shifted by $NM\ell$ samples is then

$$\text{COVAR}[C_j(NM\ell)] = E[[C_j(r) - P_j(r)]^* [C_j(r - NM\ell) - P_j(r - NM\ell)]] \quad (A.6)$$

The data samples overlap when $|\ell| < 1$. Using the relationship between the autocorrelation, $R_{nn}(kT)$, and the autospectrum, $S_{nn}(\omega)$, of the noise

$$E[n_q n_{q-k}] = R_{nn}(kT) = 1/2 \int_{-\omega_0}^{\omega_0} S_{nn}(\omega) e^{i\omega kT} d\omega \quad (A.7)$$

where $\omega_0 = \pi/T$ is the Nyquist frequency, the covariance becomes

$$\text{COVAR}[C_j(NM\ell)] = 1/[2(NM)^2] \int_{-\omega_0}^{\omega_0} S_{nn}(\omega) e^{i\omega NM\ell T} \left| \sum_{m=1}^M e^{i\omega NT(m-1)} \right|^2 \cdot \left| \sum_{k=1}^N e^{i[\omega T - (2\pi/N)(j-1)](k-1)} \right|^2 d\omega \quad (\text{A.8})$$

Using the geometric progression,

$$\text{COVAR}[C_j(NM\ell)] = 1/[2(NM)^2] \int_{-\omega_0}^{\omega_0} S_{nn}(\omega) e^{i\omega NM\ell T} [\sin(\omega NTM/2)/\sin(\omega NT/2)]^2 \cdot \{\sin[(\omega - \omega_j)NT/2]/\sin[(\omega - \omega_j)T/2]\}^2 d\omega \quad (\text{A.9})$$

where the frequency of the j^{th} harmonic is $\omega_j = (2\pi/NT)(j-1)$. The term

$$\{\sin[(\omega - \omega_j)NT/2]\}^2 / [\sin(\omega NT/2)]^2 = 1 \quad (\text{A.10})$$

since the two sine functions are offset by multiples of π . The covariance is now

$$\text{COVAR}[C_j(NM\ell)] = 1/[2(NM)^2] \int_{-\omega_0}^{\omega_0} S_{nn}(\omega) e^{i\omega NM\ell T} \cdot \{\sin(\omega NTM/2)/\sin[(\omega - \omega_j)T/2]\}^2 d\omega \quad (\text{A.11})$$

The ratio of the two sine functions is the magnitude squared of a filter, $H(\omega)$, that is placed about each ω_j

$$|H(\omega)|^2 = 1/(NM)^2 \{\sin(\omega NTM/2)/\sin[(\omega - \omega_j)T/2]\}^2 \quad (\text{A.12})$$

Without loss of generality, this filter is evaluated at $\omega_j = 0$. First, let

$$\omega = [2\pi/(NMT)]u \quad (A.13)$$

then

$$|H(u)|^2 = 1/(NM)^2 [\sin(\pi u)/\sin(\pi u/NM)]^2 \quad (A.14)$$

The magnitude squared of this filter is zero at $|u| = 1, 2, 3, \dots$, and it is a maximum at $|u| = 0, 1.5, 2.5, 3.5, \dots$. Since $\pi u/NM$ is small, the approximation is made that $\sin(\pi u/NM) = \pi u/NM$. This approximation gives a $\sin(x)/x$ filter:

$$|H(u)|^2 = [\sin(\pi u)/\pi u]^2 \quad (A.15)$$

For $|u| > 9.5$, the magnitude of the filter squared is greater than -30 dB. This filter has $M - 1$ maxima between each ω_j , where M is the number of cycles averaged. As M is increased, this filter is more and more concentrated about each ω_j . The envelope of this filter asymptotically decays as $1/(\pi u)^2$. Figure A.1 shows this filter for $M = 4$ superimposed on a noise autospectrum.

Assuming that $S_{nn}(\omega)$ is constant across each of these filters centered at ω_j , then

$$\text{COVAR}[C_j(NM\ell)] = S_{nn}(\omega_j) [2/(\pi NMT)] \int_0^{NM/2} [\sin(\pi u)/u]^2 \cos(2\pi \ell u) du \quad (A.16)$$

As discussed above, this filter rapidly decays to zero, so for NM large, the upper limit of integration is taken as infinity. With this assumption, the integral is $(1-\ell)\pi^2/2$ for $|\ell| < 1$ and zero for $|\ell| \geq 1$. Unless overlapped coefficient estimates are made, the covariance is zero.

The variance of the Fourier series coefficients is the covariance evaluated at $\ell = 0$, so

$$\text{VAR}[C_j] = S_{nn}(\omega_j) \omega_o/(NM) = S_{nn}(\omega_j) \omega_f/(2M) \quad (A.17)$$

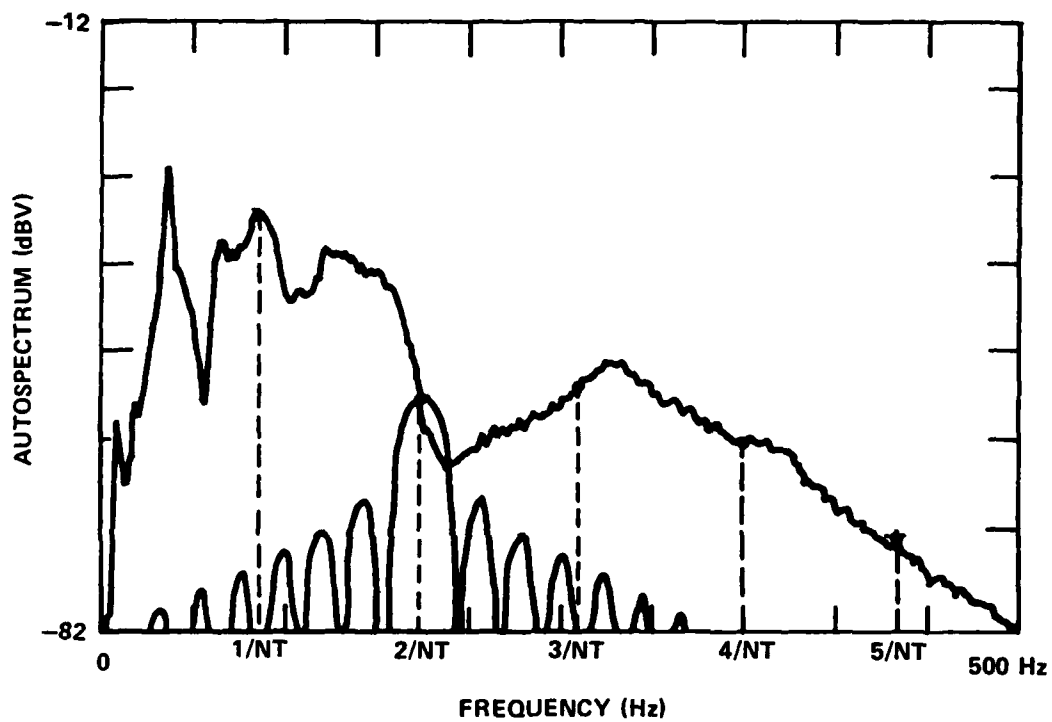


Figure A.1 - $\text{Sin}(x)/x$ Filter for $M = 4$ Superimposed on Noise Autospectrum

where $\omega_f = 2\pi/NT$ is the fundamental frequency in radians per second. The variance of C_j is the autospectrum of the noise at the harmonic frequency multiplied by the bandwidth between each harmonic. This is then divided by two times the number of cycles averaged. Signal averaging reduces the influence of the noise power by an amount that is inversely proportional to the number of cycles averaged.

When using the result given by Equation (A.17), measured spectral values are used in place of $S_{nn}(\omega)$; therefore estimates of the variance are obtained. Bias can exist in these variance estimates when the noise autospectrum varies over a wide amplitude range with frequency, and the variance is then estimated in a region where the noise spectrum is small. An example of this situation is shown in Figure A.1. The variance estimated using Equation (A.17) in this case will be smaller than the actual variance. The large, low frequency spectral levels of the noise are passed by the low frequency sidelobes of the filter.

The coefficient variance given by Equation (A.17) was compared to actual test data. This relationship is shown to be useful in estimating the variance; however, judgement is required when applying it to actual data. The results from this comparison are given in the remainder of this appendix.

The noise time history that produced the autospectrum given in Figure A.1 was sampled, signal averaged, and converted into Fourier series coefficient estimates. For each selected number of signal averages, M , this process was repeated 200 times and the variance was estimated from these 200 coefficients. Then, the autospectrum estimates from Figure A.1 were obtained for each harmonic and used with Equation (A.17).

For the first two harmonics, the results of this comparison are given in Figures A.2 and A.3; the other harmonics follow similar trends. The solid line in these figures is the predicted relationship from Equation (A.17). The results from the first harmonic compare very closely over most of the range of M . As seen in Figure A.1, most of the noise is concentrated about the first harmonic, and the spectrum is a maximum at this frequency. For $M < 6$, the measured variance falls further below the predicted line; using the spectral peak in Equation (A.1) overpredicts the variance in this region. As discussed earlier, the second harmonic is near a minimum in the noise spectrum, so the variance is underpredicted by Equation (A.1). For $M > 10$, the filter becomes "sharper" and the variance estimates more closely approach the predicted line.

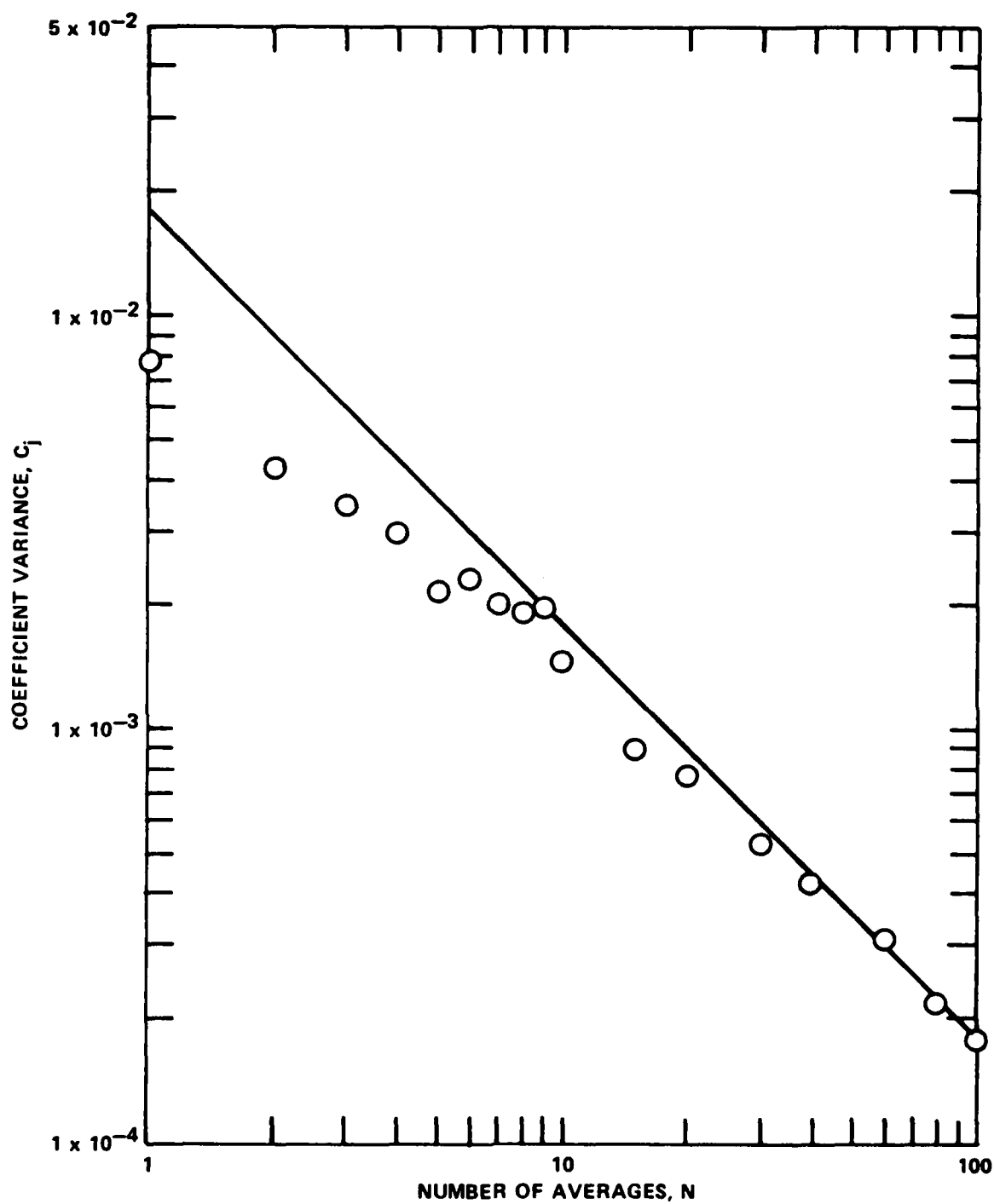


Figure A.2 - Coefficient Variance for First Harmonic

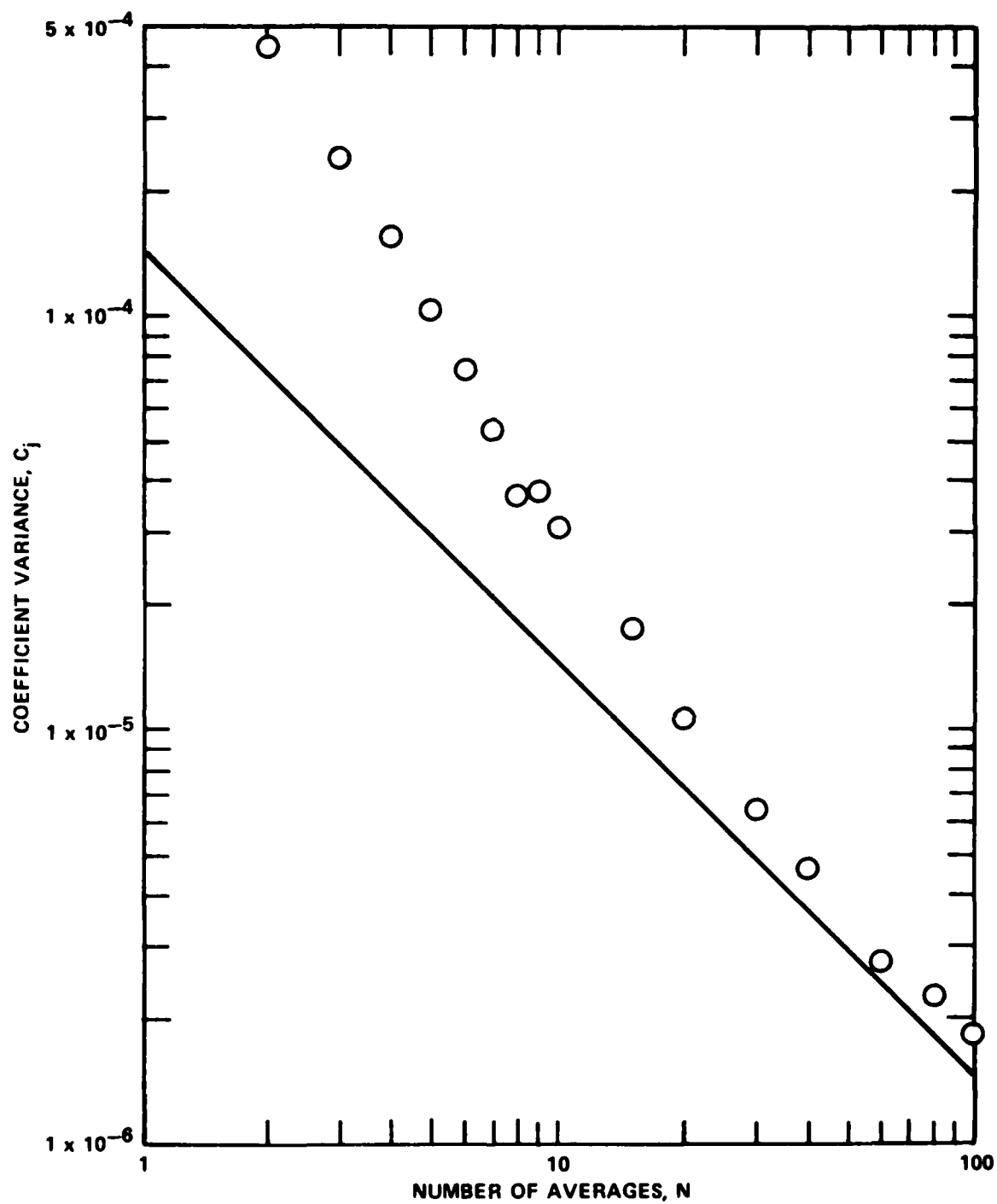


Figure A.3 - Coefficient Variance for Second Harmonic

REFERENCES

1. Chaplin, B., "Anti-Noise -- the Essex Breakthrough," Chartered Mechanical Engineer, pp. 42-47 (Jan 1983).
2. Kosaka, T. et al., "Active Noise Reduction of Low Frequency Noise in a Pipe," Proceedings of Inter-noise 84, Honolulu, Hawaii, pp. 473-476 (1984).
3. Smith, R.A. and G.B.B. Chaplin, "A Comparison of Some Essex Algorithms for Major Industrial Applications," Proceedings of Inter-Noise 83, Edinburgh, UK, pp. 407-410 (1983).
4. Widrow, B. and S.D. Stearns, Adaptive Signal Processing, Prentice Hall, Englewood Cliffs, N.J. (1985).

INITIAL DISTRIBUTION

Copies			Copies	Code	Name
2	NAVSEA		1	294	E.N. Screen
	1 SEA 55N/Harris		1	295	R.T. Schwartz
	1 SEA 55N/Wieczorek		30	2960	R.D. Pierce
12	DTIC		10	5211.1	Reports Distribution
			1	522.1	TIC (C)
			1	522.2	TIC (A)
	CENTER DISTRIBUTION				
Copies	Code	Name			
1	012	E.B. O'Neill			
1	012.3	D.D. Moran			
1	12	W.C. Dietz			
1	15	W.B. Morgan			
1	1504	V. Monacella			
1	1543	E.P. Rood			
1	16	H.R. Chaplin			
1	17	W.W. Murray			
1	19	M.M. Sevik			
1	1901	M. Strasberg			
1	1905.3	R.H. Cantrell			
1	1905.4	D. Feit			
1	194	F.S. Archibald			
1	196	D.J. Vendittis			
4	1961	B. Douglas			
1	1961	R. Evans			
1	1961	R. Ratcliffe			
1	27	R.C. Allen			
1	274	L.J. Argiro			
1	2740	Y. Wang			
1	2742	D.E. Goldsmith			
1	2742	J.E. Smith			
1	28	J.R. Belt			
5	29	G.G. Switzer			
1	2901	R.G. Stilwell			

END

FILMED

8-85

DTIC